

in time without interfering with each other. In such cases the spikes are expected to give multiple filaments at various locations across the cross section of the main beam.

One of us (N.C.K.) would like to acknowledge financial support by the Ministry of Education, Government of Japan. We thank Mr. M. Yoshizawa for help in numerical calculations.

¹Several excellent review articles have been written on self-focusing, which give details about the different models of the theory and provide extensive references. See, for example, S. A. Akhmanov, A. P. Sukhorukov, and R. V. Khokhlov, *Usp. Fiz. Nauk* **93**, 19 (1968) [*Sov. Phys. Usp.* **10**, 609 (1968)]; O. Svelto, *Prog. Opt.* **12**, 1 (1974); S. A. Akhmanov, R. V. Khokhlov, and A. P. Sukhorukov, in *Laser Handbook*, Vol. 2, edited by

F. T. Arecchi and E. O. Schulz-Dubois (North-Holland, Amsterdam, 1972), Chap. E3; V. N. Lugovoi and A. M. Prokhorov, in *Progress in Lasers and Laser Fusion*, edited by A. Perlmutter and S. M. Widmayer (Plenum, New York, 1975), p. 309; Y. R. Shen, *Prog. Quantum Electron.* **4**, 1 (1975); J. H. Marburger, *Prog. Quantum Electron.* **4**, 35 (1975).

²V. I. Bespalov and V. I. Talanov, *Pis'ma Zh. Eksp. Teor. Fiz.* **3**, 471 (1966) [*JETP Lett.* **3**, 307 (1966)].

³B. R. Suydam, in *Laser Induced Damages in Optical Materials*, U. S. NBS Special Publication No. 387, edited by A. J. Glass and A. H. Guenther (U.S. GPO, Washington, D.C., 1973); B. R. Suydam, *IEEE J. Quantum Electron.* **10**, 837 (1974).

⁴S. C. Abbi and Nitin C. Kothari, *Phys. Rev. Lett.* **43**, 1929 (1979).

⁵S. C. Abbi and Nitin C. Kothari, *J. Appl. Phys.* **51**, 1385 (1980), and **52**, 97 (1981).

⁶E. Yablonovitch and N. Bloembergen, *Phys. Rev. Lett.* **29**, 907 (1972).

From Optical Tristability to Chaos

H. J. Carmichael, C. M. Savage, and D. F. Walls

Department of Physics, University of Waikato, Hamilton, New Zealand

(Received 30 July 1982)

Numerical evidence is presented for period doubling and chaos at attainable laser powers in a model for optical tristability comprising two ring-cavity modes coupled via a $J = \frac{1}{2}$ to $J = \frac{1}{2}$ transition. A sequence of periodic windows found embedded in the chaos for this model has also been found in the Lorenz equations. It is suggested that it begins an infinite sequence of a new period-doubling type.

PACS numbers: 42.65.-k

The first, and perhaps the simplest, example of a nonlinear flow containing chaos was studied by Lorenz. Some years ago Haken observed that the single-mode laser equations may be transformed into the Lorenz equations.¹ However, the parameters required to see a chaotic laser output were unrealistic.² Recently, Ikeda has predicted that the output from a bistable ring cavity may self-oscillate and show period doubling and chaos.³ His proposal has renewed interest in nonlinear optical examples of chaotic dynamics.

Laser power requirements limit the prospects for all optical experiments based on Ikeda's proposal⁴; although in a related hybrid system⁵ both periodic and aperiodic self-oscillations have been observed.⁶ In this Letter we propose an all optical system which gives chaos at attainable laser powers.

We consider the model for optical tristability proposed by Kitano, Yabuzaki, and Ogawa⁷ and

extended by ourselves⁸ to include saturation and absorption. Two circularly polarized ring-cavity modes, with complex amplitudes E_1 and E_2 , interact via a $J = \frac{1}{2}$ to $J = \frac{1}{2}$ transition (Fig. 1) and are driven by external fields with equal amplitude E . After adiabatic elimination of the atoms, the susceptibility derived from the $J = \frac{1}{2}$ to $J = \frac{1}{2}$ inter-

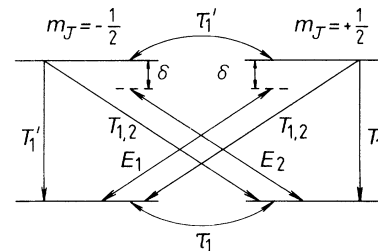


FIG. 1. Energy-level diagram for two-mode interaction with $J = \frac{1}{2}$ to $J = \frac{1}{2}$ transition.

action is the same, with a reparametrization, as that obtained in Ref. 8 by using three-level atoms and eliminating the ground-state coherence.⁹ The coupled cavity mode amplitudes obey the driven-oscillator equations,

$$\begin{aligned} \dot{\mathcal{E}}_{1,2} &= \mathcal{E} - \mathcal{E}_{1,2} [1 + i\varphi + C(1 - i\delta)(1 + |\mathcal{E}_{2,1}|^2) / S(|\mathcal{E}_1|^2, |\mathcal{E}_2|^2)], \\ S(|\mathcal{E}_1|^2, |\mathcal{E}_2|^2) &= 1 + \frac{1}{2}(1 + \eta)(|\mathcal{E}_1|^2 + |\mathcal{E}_2|^2) + \eta|\mathcal{E}_1|^2|\mathcal{E}_2|^2, \end{aligned} \quad (1)$$

with

$$\eta = \left[\left(\frac{1}{T_1} + \frac{1}{T_1'} \right)^{-1} \frac{\tau_1}{2} \right] \left(\frac{1}{\tau_1} + \frac{1}{\tau_1'} + \frac{1}{T_1'} \right) \left(\frac{2}{\tau_1'} + \frac{1}{T_1} + \frac{1}{T_1'} \right)^{-1}, \quad (2)$$

and

$$\mathcal{E}_{1,2} = \frac{2(\frac{2}{3})^{1/2} |\mu| [T_2(1/T_1 + 1/T_1')^{-1}]^{1/2}}{\hbar (1 + \delta^2)\eta} E_{1,2}, \quad \mathcal{E} = \frac{2(\frac{2}{3})^{1/2} |\mu| [T_2(1/T_1 + 1/T_1')^{-1}]^{1/2}}{\hbar} \exp(i\varphi_T) \left(\frac{\sqrt{T\mathcal{F}}}{\pi} \right) E. \quad (3)$$

Time is measured in units of the cavity decay time $\kappa^{-1} = \mathcal{F}\mathcal{L}/\pi c$, where \mathcal{L} is the cavity length and \mathcal{F} is the cavity finesse; $\tau_1/2$ and $\tau_1'/2$ are decay times for the population differences between ground- and excited-state magnetic sublevels, respectively, $(1/T_1 + 1/T_1')^{-1}$ is the excited-state lifetime, and T_2 is the decay time for the optical dipole coherences; μ is the reduced atomic dipole matrix element; $\delta = T_2\delta\omega$ and $\varphi = \kappa^{-1}\Delta\omega$ are atomic and cavity detunings (equal for each mode), and $C = (1 + \delta^2)^{-1}\alpha L\mathcal{F}/4\pi$, where α is the resonant absorption coefficient and L is the propagation distance in the medium; T is the transmission coefficient, and φ_T the accompanying phase shift at the cavity input mirror.

We will define $Y = |\mathcal{E}|^2$ and $X_{1,2} = |\mathcal{E}_{1,2}|^2$. In Fig. 2 we plot the steady-state solutions for $X_{1,2}$ as a function of Y for fixed C , δ , φ , and η . The inset features the transition to optical tristability—one symmetric and two asymmetric branches.⁷ Beyond this weak-field regime the asymmetric branches undergo a Hopf bifurcation. In Ref. 8

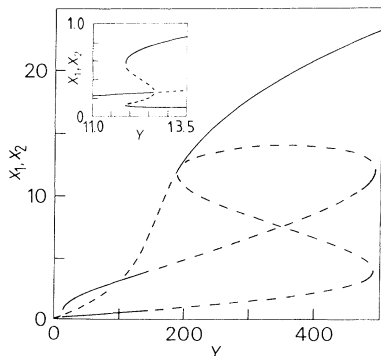


FIG. 2. Steady-state intensities X_1 and X_2 vs Y for $C = 4$, $\delta = 5$, $\varphi = 15$, and $\eta = 0.03$. Solid (dashed) lines denote stable (unstable) states.

we found this behavior in the dispersive limit. It is retained here in the presence of both absorption and dispersion. For $145 < Y < 185$ all three steady states are unstable and therefore some form of self-oscillatory output is assured. Indeed, we have numerically integrated Eqs. (1), and just beyond the Hopf bifurcation point all trajectories are attracted to simple limit cycles enclosing each unstable asymmetric fixed point. At larger values of Y we find chaos.

Before this system can be judged as a candidate for experiments we require some indication of the parameter range over which chaotic dynamics might be observed. Only then can power and stability requirements be estimated. To this end we have carried out a survey in (Y, φ) space. We stepped Y in units of 1 and φ in units of 0.1 to generate the map shown in Fig. 3. The attractor identified at each point is represented by a square centered at that point. In addition to achieving our stated objective this survey has uncovered a result of more fundamental interest. Several periodic windows found embedded in the chaos appear to begin an infinite sequence of a new period-doubling type. We have verified that this

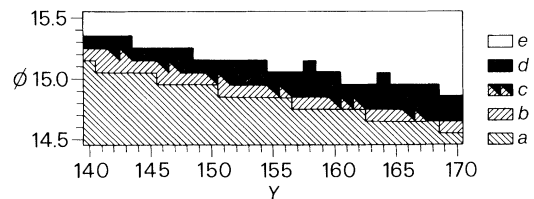


FIG. 3. Map of attractors in (Y, φ) space for $C = 4$, $\delta = 5$, and $\eta = 0.03$: (a) fixed point; (b) limit cycles encircling each unstable asymmetric fixed point; (c) hysteresis; (d) chaos; (e) assorted limit cycles encircling both unstable asymmetric fixed points.

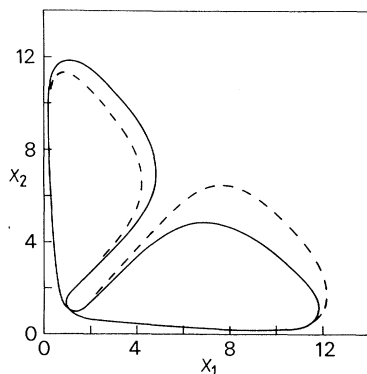


FIG. 4. Symmetric and asymmetric limit cycles in the approach to chaos from above: $C = 4$, $\delta = 5$, $\varphi = 15$, $\eta = 0.03$, and $Y = 170$ (solid curve), $Y = 166$ (dashed curve).

sequence, though previously unreported, occurs also in the Lorenz equations. We will review these findings first.

In Fig. 3 the chaotic region is bounded below by a transition, with hysteresis, between the stable limit cycles encircling each asymmetric fixed point and an aperiodic attractor encircling both (see Fig. 6). A similar hysteresis occurs in the Lorenz equations, although there is no preliminary Hopf bifurcation and the transition is between an aperiodic attractor and stable fixed points.¹⁰ In the unshaded portion of Fig. 3 our survey turned up an assortment of stable cycles encircling both asymmetric fixed points. A closer look reveals the following approach to the chaotic region from above: (1) A symmetric cycle (solid curve in Fig. 4) bifurcates to a pair of asymmetric cycles (dashed curve in Fig. 4 and its reflection about $X_1 = X_2$). (2) Each asymmetric cycle period doubles to chaos (Fig. 5). (3) The two asymmetric aperiodic attractors so formed merge on a symmetric aperiodic attractor (Fig. 6). This is again analogous to behavior in the Lorenz equations.¹⁰ Continuing into the chaotic region we have found numerical evidence suggesting that the development shown in Figs. 4–6 merely represents the first in an infinite sequence of such bifurcations to chaos. The further members of this sequence appear as periodic windows embedded in the chaotic region. The two-looped and four-looped cycles in Fig. 7 were found in our survey. They each bifurcate to chaos via the foregoing steps. Then, assuming a geometric convergence of successive periodic windows we have looked for and found an eight-looped cycle at $Y = 160.44$. Moreover, we have found the same sequence, up to this eight-looped stage, in the

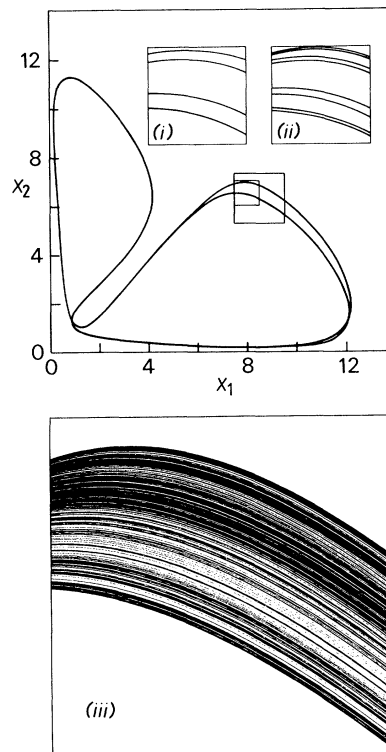


FIG. 5. Period doubling to chaos from asymmetric cycle in Fig. 4: $C = 4$, $\delta = 5$, $\varphi = 15$, $\eta = 0.03$, and $Y = 165$; (i) $Y = 164.9$, (ii) $Y = 164.88$, (iii) $Y = 164.8$.

Lorenz equations. Note that each new symmetric cycle looks like a superposition of two asymmetric versions of its predecessor. This suggests a new period-doubling mechanism involving a merging of these three cycles on a homoclinic orbit.

From Eq. (3) the total laser power density is

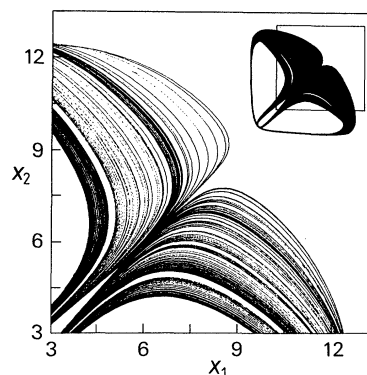


FIG. 6. Aperiodic attractor for $C = 4$, $\delta = 5$, $\varphi = 15$, $\eta = 0.03$, and $Y = 163.7$.

given by

$$P = \left(\frac{4\pi^4 \hbar c}{\lambda^3} \times 10^{-4} \right) \left[\frac{T_R}{(1/T_1 + 1/T_1')^{-1} T_2} \right] \eta (1 + \delta^2) T^{-1} \mathfrak{F}^{-2} Y \quad (4)$$

in W cm^{-2} , where $|\mu|$ has been expressed in terms of the radiative lifetime T_R and λ is the wavelength of the atomic transition. We base our estimate of P on the D_1 line of sodium using 1600 MHz of collisional broadening to average over the hyperfine structure. We initially assume $T_R = (1/T_1 + 1/T_1')^{-1}$ and $\mathfrak{F} = \pi/T$, and with $T_2 = 100$ psec, $\lambda = 5.9 \times 10^{-5}$ cm, $\mathfrak{F} = 200$, $\delta = 5$, and $\eta = 0.03$ we find $P = 6.3Y$ mW cm^{-2} . Then the values of Y in Fig. 3 correspond to minimal power requirements, of the order of 1 W cm^{-2} . In the presence of intracavity and mirror transmission losses ($\mathfrak{F} \neq \pi/T$) this estimate is multiplied by $\pi/\mathfrak{F}T$ (an order of magnitude if resonant empty-cavity transmission is reduced to 1%).

With rapid depolarization of the excited state ($\tau_1' \ll \tau_1, T_1, T_1'$) and $T_2 = 100$ psec, $\eta = 0.03$ implies $\tau_1/2 = 270$ nsec. Then setting $\kappa^{-1} = \tau_1/2$ (111.5-cm cavity with $\mathfrak{F} = 200$) we obtain $\Delta\varphi = 2\pi\kappa^{-1}\Delta f = 0.17$ for a laser frequency jitter Δf

$= 100$ kHz. This provides the frequency stability required to resolve the chaotic region in Fig. 3.

These estimates are very optimistic. However, they require some qualification. The present theory adiabatically eliminates the atoms and includes only a single longitudinal cavity mode. This imposes the restriction

$$\kappa^{-1} \gg \tau_1/2, \tau_1'/2, (1/T_1 + 1/T_1')^{-1}, T_2 \gg \mathfrak{L}/2\pi c. \quad (5)$$

We have set $\kappa^{-1} = \tau_1/2$, and while chaos may persist under these conditions, to strictly justify adiabatic elimination of the atoms either the atoms must relax faster or the cavity slower. Quenching the atomic decay and lowering $\tau_1/2$ accordingly will raise the power requirement by $T_R/(1/T_1 + 1/T_1')^{-1}$. Alternatively, better frequency stability and correspondingly higher cavity finesse lowers the power required. Also, while 1600 MHz of collisional broadening convincingly averages the sodium hyperfine structure, to justify the single-mode assumption T_2 should strictly be increased by an order of magnitude ($\mathfrak{L}/2\pi c = 590$ psec). While this reduces the power requirement accordingly, the effect of the hyperfine structure becomes more uncertain. Of course, an alternative atomic system might circumvent this problem.

This work has been supported in part by the United States Army through its European Research Office.

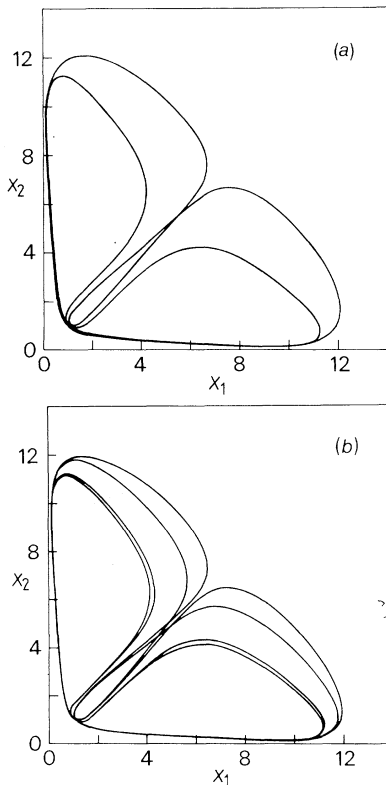


FIG. 7. Symmetric limit cycles from two periodic windows embedded in the chaos: $C = 4$, $\delta = 5$, $\varphi = 15$, $\eta = 0.03$, and (a) $Y = 163.6$, (b) $Y = 161$.

¹H. Haken, Phys. Lett. **53A**, 77 (1975).

²Period doubling to chaos in an inhomogeneously broadened single-mode laser has recently been reported by N. B. Abraham, M. D. Coleman, M. Maeda, and J. C. Wesson, Appl. Phys. **B28**, 169 (1982).

³K. Ikeda, Opt. Commun. **30**, 257 (1979).

⁴R. R. Snapp, H. J. Carmichael, and W. C. Schieve, Opt. Commun. **40**, 68 (1981).

⁵K. Ikeda, H. Daido, and O. Akimoto, Phys. Rev. Lett. **45**, 709 (1980).

⁶H. M. Gibbs, F. A. Hopf, D. L. Kaplan, and R. L. Shoemaker, Phys. Rev. Lett. **46**, 474 (1981).

⁷M. Kitano, T. Yabuzaki, and T. Ogawa, Phys. Rev. Lett. **46**, 926 (1981).

⁸C. M. Savage, H. J. Carmichael, and D. F. Walls, Opt. Commun. **42**, 211 (1982).

⁹M. W. Hamilton, R. J. Ballagh, and W. J. Sandle, to be published.

¹⁰R. Gilmore, *Catastrophe Theory for Scientists and Engineers* (Wiley, New York, 1981), pp. 553–62.